



Research article

High-content screening of active components of Traditional Chinese Medicine inhibiting TGF- β -induced cell EMT



Mengzhen Xu^{a,1}, Qinghua Cui^{b,1}, Wen Su^b, Dan Zhang^c, Jiayu Pan^a, Xiangqi Liu^b, Zheng Pang^{b,*}, Qingjun Zhu^{b,d,**}

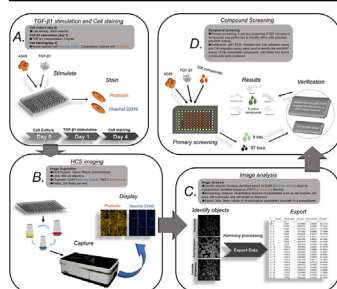
^a College of Pharmaceutical Science, Shandong University of Traditional Chinese Medicine, Jinan 250355, China

^b Innovative Institute of Chinese Medicine and Pharmacy, Shandong University of Traditional Chinese Medicine, Jinan 250355, China

^c Experimental Center, Shandong University of Traditional Chinese Medicine, Jinan 250355, China

^d Key Laboratory of Traditional Chinese Medicine Classical Theory, Ministry of Education, Shandong University of Traditional Chinese Medicine, Jinan 250355, China

GRAPHICAL ABSTRACT



ARTICLE INFO

Keywords:

High-content screening
Epithelial-mesenchymal transition
Traditional Chinese Medicine
TGF- β 1

ABSTRACT

The epithelial mesenchymal transition (EMT) has roles in metastasis and invasion during fibrotic diseases and cancer progression. Some Traditional Chinese Medicines (TCMs) have shown inhibitory effects with respect to the EMT. The current study attempted to establish a multiparametric high-content method to screen for active monomeric compounds in TCM with the ability to target cellular EMT by assessing phenotypic changes. A total of 306 monomeric compounds from the MedChemExpress (MCE) compound library were screened by the high-content screening (HCS) system and 5 compounds with anti-EMT activity, including camptothecin (CPT), dimethyl curcumin (DMC), artesunate (ART), sinapine (SNP) and berberine (BER) were identified. To confirm anti-EMT activity, expression of EMT markers was assessed by qRT-PCR and Western blotting, and cell adhesion and migration measured by cell function assays. The results revealed that CPT, DMC, ART, SNP and BER inhibited transforming growth factor- β 1 (TGF- β 1)-induced expression of vimentin and α -SMA, upregulated expression of E-cadherin, increased cell adhesion and reduced cell migration. In summary, by quantifying the cell morphological changes during TGF- β 1-induced EMT through multi-parametric analysis, TCM compounds with anti-EMT activity were successfully screened using the HCS system, a faster and more economical approach than conventional methods.

* Corresponding author.

** Corresponding author.

E-mail addresses: 60230021@sduetcm.edu.cn (Z. Pang), zhuqingjuncn@hotmail.com (Q. Zhu).

¹ These authors contributed equally to this work.

<https://doi.org/10.1016/j.heliyon.2022.e10238>

Received 25 February 2022; Received in revised form 13 May 2022; Accepted 5 August 2022

2405-8440/© 2022 The Author(s). Published by Elsevier Ltd. This is an open access article under the CC BY-NC-ND license (<http://creativecommons.org/licenses/by-nc-nd/4.0/>).

1. Introduction

The epithelial mesenchymal transition (EMT) is a biological process that allows epithelial cells to acquire mesenchymal cell phenotypes and has roles in embryonic development, cancer metastasis and fibrotic diseases [1, 2, 3, 4]. During the EMT, tight junctions between epithelial cells are lost and the cells lose apical-basal polarity and acquire a highly migratory and invasive mesenchymal cell phenotype [5, 6, 7]. In addition, cells undergo cytoskeletal reorganization and the morphology changes from pebble-like to spindle-like [8, 9]. The EMT process can be triggered by a variety of growth factors, including transforming growth factor- β (TGF- β) [10].

Traditional Chinese Medicine (TCM) has been used to suppress the EMT and has few side effects and high efficacy. For instance, baicalin from *Scutellaria baicalensis* has been used to impede the EMT via inhibition of the PDK1/AKT pathway in human non-small-cell lung cancer (NSCLC) [11]. Gallic acid, which is present in a number of fruits, exerts an anti-EMT effect by regulation of the TGF- β /Smad pathway [12]. Andrographolide, one of the active ingredients of *Andrographis paniculata*, also regulates the TGF- β /Smad pathway [13]. Astragalus polysaccharide from *Astragalus* species increases E-cadherin expression and suppresses expression of Vimentin and α -SMA, leading to inhibition of the EMT and improved collagen deposition [14]. However, TCM is composed of complex ingredients with multiple targets so that systematic screening for compounds with anti-EMT activity requires time-consuming and costly pharmacological assays which are unsuitable for large-scale operation. Therefore, there is an urgent need to establish a rapid and reliable high-throughput screening method to identify monomeric components of TCM with anti-EMT activity.

High-content screening (HCS) detects fluorescently labeled cell markers by microscopic imaging, analysis of which reveals molecular activity inside the cells [15]. The result is high-quality information on cell morphology and structure harvested from qualitative and quantitative evaluation of microscopic images. In addition, the HCS software can automatically perform qualitative and quantitative analysis of different cellular features. This powerful imaging and analysis system makes the HCS suitable for cell research [16, 17, 18].

The current study evaluated cellular phenotypic changes via a multiparametric, high-throughput method in order to screen monomeric components of TCM for anti-EMT activity. The A549 cell-line, from type II alveolar epithelial cells, is commonly used for studying the TGF- β -induced EMT *in vitro* [19, 20, 21]. Following the multiparametric analysis of morphological changes during the TGF- β -induced EMT via the HCS system, principal component analysis (PCA) was used to reduce the number of parameters and establish an evaluation system based on cell morphological changes. The anti-EMT activity of a specific monomer may be evaluated from the distribution area on a PCA score plot. A total of 306 monomeric compounds were screened for anti-EMT activity by this method and camptothecin (CPT), dimethyl curcumin (DMC), artemisinin (ART), sinapine (SNP) and berberine (BER) were identified as having activity. Expression of EMT markers in A549 cells was assessed by qRT-PCR and Western blotting and cell adhesion and migratory ability were measured. CPT, DMC, ART, SNP and BER all increased E-cadherin (epithelial cell marker) expression while the expression of Vimentin (mesenchymal cell marker) and α -SMA (fibroblast marker) was decreased. All compounds were also found to enhance cell adhesion and decrease cell migration. DMC and SNP are identified as novel inhibitors of the TGF- β -induced EMT in A549 cells. In summary, a screening method based on the HCS system was established to screen compounds with anti-EMT activity by analyzing cellular morphology changes. The current report is of a novel approach for the screening of active components of TCM with EMT-inhibitory activity.

2. Materials and methods

2.1. Cell culture

A549 cells (Procell, Wuhan, China) were cultured in RPMI-1640 (Gibco, Sigma Aldrich, Denmark) containing 10% fetal bovine serum (FBS, Gibco, Sigma Aldrich, Denmark), 100 U/ml penicillin and 100 μ g/ml streptomycin (Gibco, Sigma Aldrich, Denmark) at 37 °C. Cells were digested with 0.25% trypsin (Gibco, Sigma Aldrich, Denmark) and passaged at 80% confluence.

2.2. Cell staining

A549 cells were seeded into a black 96-well plate (PerkinElmer, Waltham, MA, USA) at a density of 3000 cells/well and cultured at 37 °C with 5% CO₂. After 24 h, cells were divided into 4 groups: Control (cell culture medium with 1% FBS and without TGF- β 1); TGF- β 1-treated (cell culture medium with 1% FBS and containing 5 ng/ml TGF- β 1); SB-431542-treated (cell culture medium with 1% FBS and containing 5 ng/ml TGF- β 1 and 10 μ M SB-431542); Compound-treated (cell culture medium with 1% FBS and containing 5 ng/ml TGF- β 1 and 10 μ M monomeric compounds). Plates were incubated at 37 °C with 5% CO₂ for 72 h. After incubation, 100 μ l of pre-warmed 4% paraformaldehyde (Solarbio, Beijing, China) was added to each well and fixed at 37 °C for 15 min. Cells were permeabilized with 0.1% Triton X-100 (Solarbio, Beijing, China) for 5 min and incubated with tetramethyl rhodamine isothiocyanate (TRITC)-phalloidin cytoskeletal staining solution (100 nM, Solarbio, Beijing, China) for 30 min. Nuclei were stained with Hoechst 33342 (100 nM, Solarbio, Beijing, China) for 30 s. Image acquisition was performed using Opera Phoenix HCS system (PerkinElmer, Waltham, MA, USA).

2.3. Image acquisition and processing

TRITC Phalloidin allows staining of the cytoskeleton and Hoechst 33342 stains nuclei. Images (200 elds per well) were acquired using the Opera Phoenix HCS system with a 40 \times objective with excitation of channel 1 at 540 nm to detect the cytoskeleton stained yellow by TRITC Phalloidin. The excitation of channel 2 was set at 346 nm to detect the nuclei stained blue by Hoechst 33342. Images were analyzed using Harmony software (PerkinElmer, Waltham, MA, USA), which quantifies morphological parameters such as cell area, cell roundness, cell length and cell number and automatically records mean values for each well.

2.4. Primary screening

A total of 306 compounds from the MedChemExpress (MCE) compound library were tested. An equal volume of medium was added to the outermost wells to avoid edge effects in the 96-well plate. Compounds were initially screened at a concentration of 10 μ M and cells counted to assess cytotoxicity. Compounds were considered cytotoxic to A549 cells if cell numbers were reduced by 50% compared with controls. Parameters of cell area, cell roundness and cell length were selected to assess cytoskeletal remodeling during the EMT. PCA is applied to reduce the dimensionality of multiple variable parameters, such as cell area, cell roundness and cell length. The PCA score plot converts the cell morphology parameters into points for visual observation. Distances between points reflect degrees of similarity between compounds: the shorter the distance, the greater the similarity. If the distribution regions of a compound are close to the control, the compound may have anti-EMT activity. Accuracy and reproducibility of results are crucial to high-throughput screening experiments. The Z' factor reflects both the assay signal dynamic range and data variation associated with signal

Table 1. Primer sequences for use in qRT-PCR.

Target	Sequence
β-actin	Forward 5'-CATCCGTAAGACCTCTATGCCAAC-3'
	Reverse 5'-ATGGAGCCACCGATCCACA-3'
Vimentin	Forward 5'-AAAGCGTGGCTGCCAAGAA-3'
	Reverse 5'-ACCTGTCTCCGTACTCGTTGA-3'
E-cadherin	Forward 5'-CAGATGATGATACCCGGGACAA-3'
	Reverse 5'-TGCAGCTGGCTCAAATCAAAG-3'
α-SMA	Forward 5'-GACAATGGCTCTGGGCTCTGTA-3'
	Reverse 5'-TTTGGCCATTCCAACCATTA-3'

measurements for assay quality assessment. The Z' factor was calculated using Eq. (1) [22].

$$Z' \text{ factor} = 1 - \frac{3(\sigma_p + \sigma_n)}{|\mu_p - \mu_n|} \quad (1)$$

where σ is the sample variance, μ is the average value, p is the positive control and n is the negative control. The current study adopted SB-431542 as the positive drug and the untreated sample as negative con-

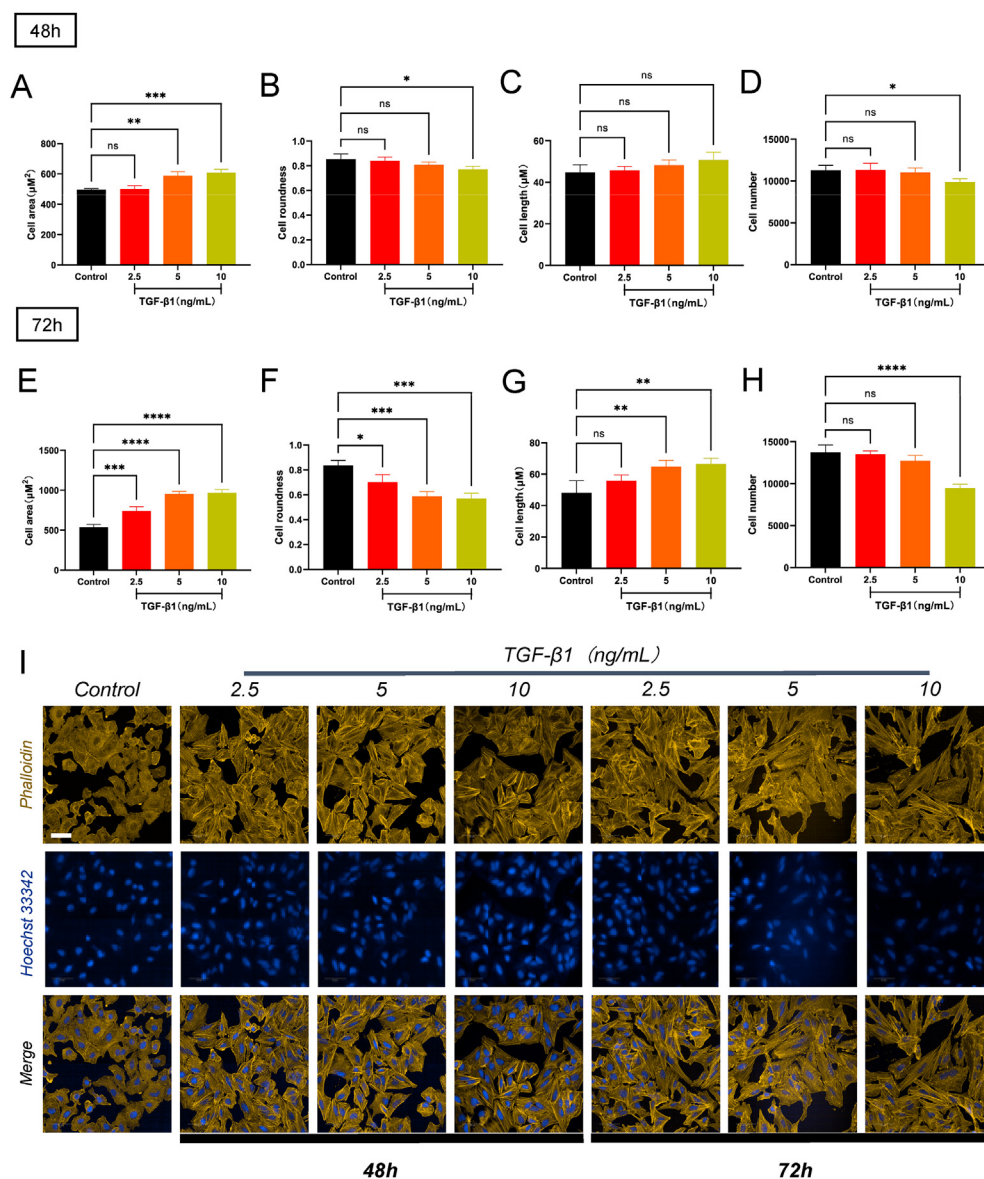
trol. If the Z' factor is between 0.5 and 1, it may be concluded that the HCS screening results are reliable and reproducible.

2.5. qRT-PCR assay

Total RNA was extracted from A549 cells using Trizol reagent (Takara, Beijing, China) and RNA was reverse-transcribed into cDNA using Prime Script[®] RT reagent kit with gDNA Eraser (Takara, Beijing, China), according to the manufacturer's instructions. mRNA expression levels were determined by qRT-PCR using a QuantStudio[™] 5 qRT-PCR system (Thermo Fisher, Waltham, MA, USA). Expression levels of E-cadherin, Vimentin and α-SMA were normalized to β-actin. Primer sequences are listed in Table 1.

2.6. Western blotting

For protein extraction and quantification, cells were washed with PBS (Solarbio, Beijing, China) and lysed in RIPA buffer containing 1% phenylmethylsulfonyl fluoride (PMSF) and 1% phosphatase inhibitor (Beyotime, Beijing, China). Samples were centrifuged at 13,000 × g for 15 min at 4 °C and supernatants collected for Western blot analysis.



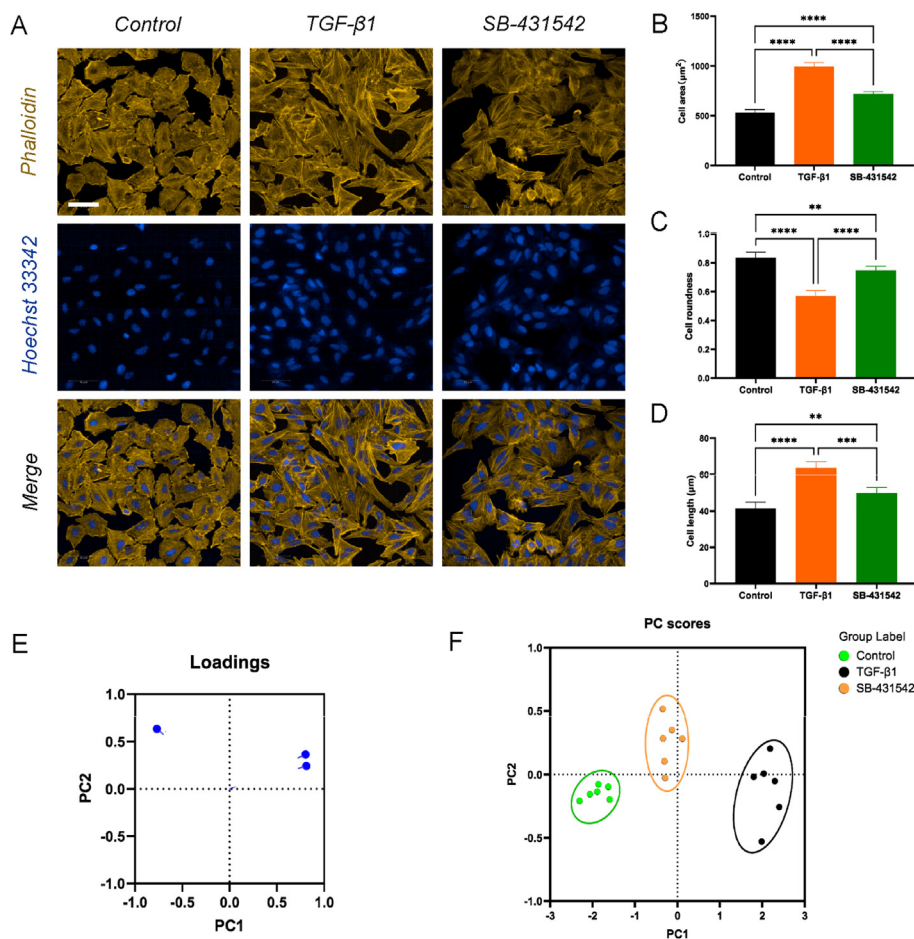


Figure 2. Establishing a screening method based on the HCS system. A549 cells were seeded into 96-well plates at a density of 3000 cells/well. After 24 h, cells were divided into 3 groups: Control (cell culture medium with 1% FBS and without TGF- β 1), TGF- β 1-treated (cell culture medium with 1% FBS and containing 5 ng/ml TGF- β 1), SB-431542-treated group (cell culture medium with 1% FBS and containing 5 ng/ml TGF- β 1 and 10 μM SB-431542). After 72 h, the cytoskeleton was stained with TRITC Phalloidin and nuclei with Hoechst 33342. Images (200 fields per well) were acquired using the Opera Phoenix HCS system (Perkin Elmer) with a 40 \times objective. Images were identified and segmented using Harmony software to quantify morphological parameters, such as cell area, cell roundness and cell length. (A) Representative stained images of A549 cells after 72 h of different treatments. Cytoskeleton stained with Phalloidin (yellow) and nuclei stained with Hoechst 33342 (blue). Scale bar = 50 μm . (B–D) Changes in cell area (B), cell roundness (C) and cell length (D) of A549 cells after stimulation with different solutions for 72 h (means \pm SEM; n = 6; *p < 0.05; **p < 0.01; ***p < 0.001; ****p < 0.0001). (E) PCA loading plot of cell area, cell roundness and cell length. (F) PCA score plot of A549 cells after 72 h of stimulation with different treatments: Control: green; TGF- β 1: black; SB-431542: orange.

Protein concentration was measured by BCA protein assay (Beyotime, Beijing, China) and 30 μg proteins separated by SDS-PAGE and transferred to a 0.45 μm PVDF membrane (Millipore, MA, USA). After blocking with 5% bovine serum albumin (BSA), the membrane was incubated with the primary antibody at 4 $^{\circ}\text{C}$ overnight. The membrane was washed and incubated with horseradish peroxidase (HRP)-labeled goat anti-rabbit IgG (H + L) or HRP-labeled goat anti-mouse IgG (H + L) (1:2000; Beyotime, Beijing, China) for 1 h at room temperature. Immunoblots were analyzed by enhanced ECL and images acquired with an Amersham Imager (General Electric, Boston, MA, USA) and quantified by densitometry (Image J 1.8.0 software). Bands were normalized to the loading control, β -actin.

2.7. Migration assay

A549 cells (2.5×10^5 cells/ml) were seeded into 6-well plates (Corning, NY, USA) and incubated for 24 h. Cells were scratched with a sterile pipette tip and washed three times with PBS. The corresponding serum-free cell culture medium was added to the cells of different groups followed by incubation for 72 h, as described in section 2.3. Between 0 to 72 h, changes to the scratched area were recorded with Digital Phase Contrast (DPC) mode under a 10 \times objective by the real-time dynamic detection function of Opera Phoenix HCS system. DPC mode allows cells to be digitally processed and clear images obtained with bright and dark contrast. The scratched area was quantified at different time points using Harmony software. Cell migration was calculated using Eq. (2) [23].

$$M = (S_a - S_e) / S_a \quad (2)$$

in which M = migration, S_a = Cell scratch area at 0 h, S_e = Cell scratch area at 72 h.

2.8. Adhesion assay

A549 cells (1.5×10^5 cells/ml) were seeded into 6-well plates and incubated for 24 h before appropriate medium containing 1% FBS was added for the respective groups (see section 2.3) and cells were further incubated for 72 h. Fibronectin (FN; 0.2 mg/ml, Solarbio, Beijing, China) was diluted with PBS and added to 96-well plates to give a final concentration of 2 $\mu\text{g}/\text{cm}^2$, dried at room temperature for 45 min and aspirated at 4 $^{\circ}\text{C}$ overnight. Cells were harvested from the 6-well plates and inoculated into the pretreated 96-well plates and incubated for 30 min at 37 $^{\circ}\text{C}$ for staining. Cells were fixed with 4% formaldehyde solution for 10 min at room temperature and permeabilized with 0.5% Triton X-100 solution for 5 min. Nuclei were stained for 30 s with 50 μl Hoechst 33342, to give a final concentration of 100 nM. Images (50 fields per well) were acquired using the Opera Phoenix HCS system with a 20 \times objective. The number of adherent cells was recorded using Harmony software.

2.9. Statistical analysis

All statistical analysis was performed with GraphPad Prism software version 9.0. Data are expressed as mean \pm standard error of the mean (SEM). Comparison between groups was analyzed by one-way analysis of variance (ANOVA) or Student's t-test. A value of p < 0.05 was considered to indicate statistical significance.

3. Results

3.1. Determination of TGF- β 1 stimulation conditions

During the stimulation of the EMT by TGF- β 1, lung epithelial cells gradually change into mesenchymal cells, resulting in increased cell area,

Table 2. Z' factor for different morphological parameters.

	Cell Area	Cell roundness	Cell length
Z' Factor	0.53	0.57	0.55

elongated cytoskeleton and a morphological shift from pebble-like to spindle-like. The HCS system was used to evaluate morphological changes in order to determine the optimal TGF- β 1 concentration to stimulate the EMT in A549 cells. No significant differences in cell area, roundness and length were observed at 2.5 ng/ml TGF- β 1 compared with controls at 48 h or 72 h but significant changes were seen with 5 ng/ml TGF- β 1. Cell morphology became more spindle-like, showing characteristics of mesenchymal cells. Changes in cell area, roundness and length were observed with 10 ng/ml TGF- β 1 at 72 h compared with controls but cell numbers were also significantly reduced, indicating cytotoxicity at this concentration (Figure 1). Based on the above results, the optimal stimulatory TGF- β 1 concentration was determined to be 5 ng/ml and the optimal stimulation time 72 h.

3.2. Establishment of a screening method based on the HCS system

A method to quantify cell morphological changes during the EMT based on the HCS system was established and cell morphology evaluated by PCA. SB-431542 selectively inhibits the activin receptor-like kinase (ALK) receptor and blocks the TGF- β 1-induced EMT. The inhibitor was used as a reference compound to verify the accuracy and reliability of the

PCA morphology scoring system [24]. Combining cell staining images and quantitative morphological analysis showed that cells in the SB-431542-treated group were mostly pebble-like with a typical epithelial cell phenotype. By contrast, cells in the TGF- β 1-treated group had increased area, decreased roundness and elongated cytoskeleton compared with the control group and evinced a morphology that was mostly spindle-like. Cells in the SB-431542-treated group had smaller area, increased roundness and a cytoskeleton and morphology that were similar to those of controls. The PCA score plot separated cells in the control and TGF- β 1-treated groups in the PC1 direction without crossover or overlap. The separation of cells in the SB-431542-treated and control groups was small. This finding was consistent with results of quantitative analysis of cell morphology, suggesting that the established PCA morphology scoring system is accurate and reliable (Figure 2). Furthermore, Z' factors for different morphological parameters indicate that our method is reproducible and suitable for high-throughput detection (Table 2).

3.3. Primary screening of monomeric compounds with anti-EMT activity

A total of 306 compounds from the MCE compound library were screened by a method based on the HCS system and a layout of the distribution of the different compounds in the 96-well plates drawn (Figure 3B). Thirty-seven compounds exhibited cytotoxicity to A549 cells (Figure 3C). The remaining compounds were plotted on a PCA score plot which converts cell morphology data into visually observable points with the distance between points reflecting the degree of

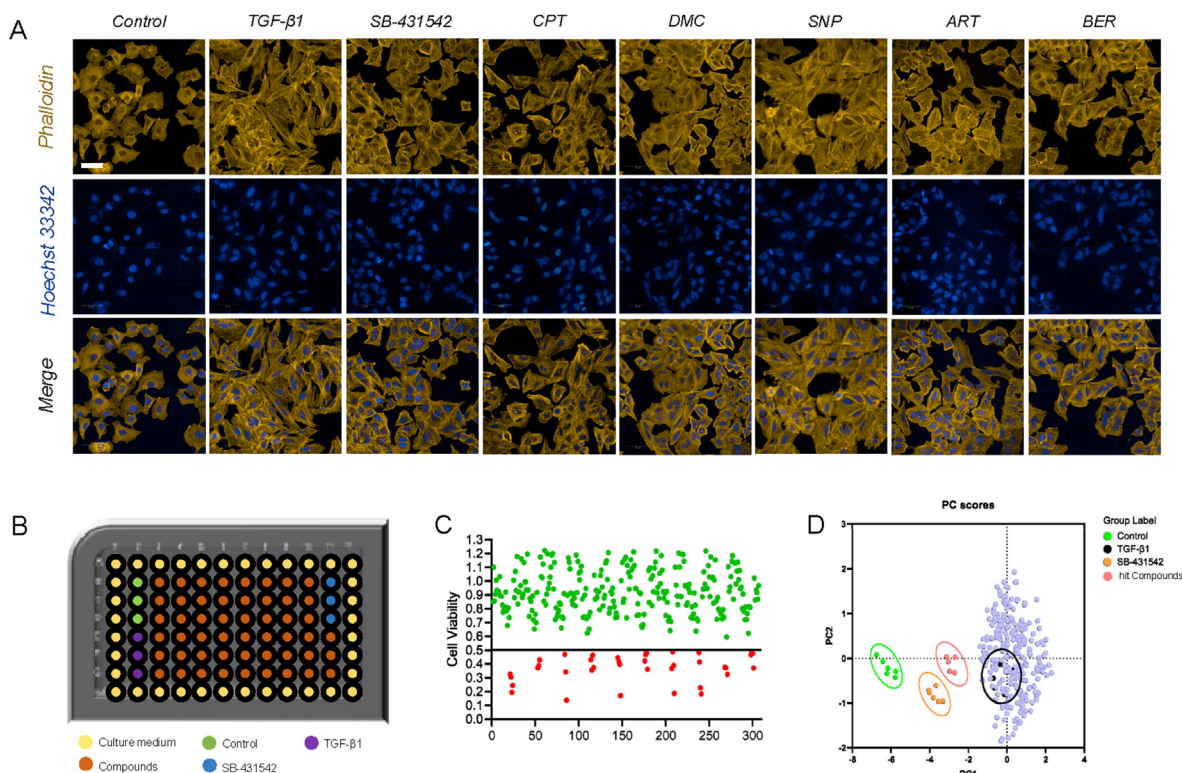


Figure 3. Results of primary screening of monomeric TCM compounds. A549 cells were seeded into 96-well plates at a density of 2000 cells/well. After 24 h, the cells were divided into 4 groups: Control (cell culture medium with 1% FBS and without TGF- β 1), TGF- β 1-treated group (cell culture medium with 1% FBS and containing 5 ng/ml TGF- β 1), SB-431542-treated group (cell culture medium with 1% FBS and containing 5 ng/ml TGF- β 1 and 10 μ M SB-431542), Compound-treated group (cell culture medium with 1% FBS and containing 5 ng/ml TGF- β 1 and 10 μ M monomeric compounds). After 72 h, the cytoskeleton was stained with TRITC Phalloidin and nuclei with Hoechst 33342. Images (200 fields per well) were acquired using the Opera Phoenix HCS system with a 40 \times objective. Images were identified and segmented using Harmony software to quantify morphological parameters, such as cell area, cell roundness, cell length and cell number. (A) Representative stained images of A549 cells after treatment with different compounds. Cytoskeleton stained with Phalloidin (yellow) and nuclei stained with Hoechst 33342 (blue). Scale bar = 50 μ m. (B) Distribution of TCM monomeric compounds in 96-well plates. (C) A549 cell viability after treatment with 306 monomeric compounds at 10 μ M for 72 h. Cytotoxic compounds: red; Non-cytotoxic compounds: green. (D) PCA score plot demonstrating the effect of different compounds on morphological scores of TGF- β 1-stimulated A549 cells: Control: green; TGF- β 1: black; SB-431542: orange; Active compounds: pink; Inactive compounds: purple.

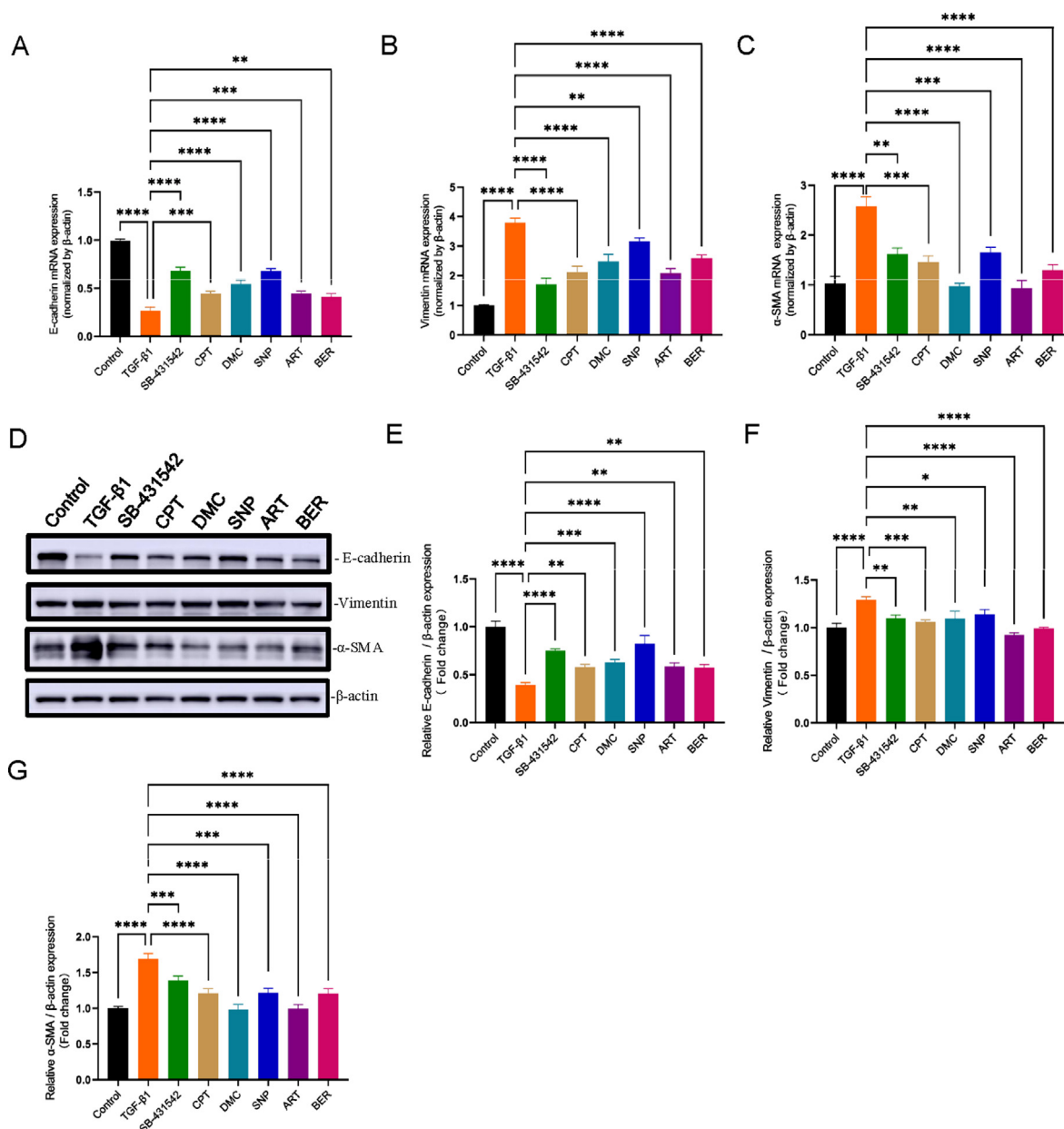


Figure 4. Expression of EMT-related markers after treatment with monomeric compounds. A549 cells were treated with different monomeric compounds for 72 h. (A–C) Expression of E-cadherin (A), Vimentin (B) and α -SMA; (C) mRNA after 72 h incubation of A549 cells with different monomeric compounds (means \pm SEM; n = 6; *p < 0.05; **p < 0.01; ***p < 0.001; ****p < 0.0001). (D) Representative Western blot images: β -actin was used as a loading control and the blots are the result of three separate experiments. For the original blots of E-cadherin, Vimentin, α -SMA and β -actin, refer to supplementary figure S2. (E–G) The expression of E-cadherin (E), Vimentin (F) and α -SMA (G) proteins after 72 h incubation of A549 cells with different monomeric compounds (means \pm SEM; n = 3; *p < 0.05; **p < 0.01; ***p < 0.001; ****p < 0.0001).

similarity between the compounds (the closer the distance, the greater the similarity). The control and the TGF- β 1-treated groups were found to have clean separation in the PC1 direction. Interestingly, 5 monomeric TCM components, CPT, DMC, ART, SNP and BER, added to cells that had not been treated with SB-431542, showed separation from the TGF- β 1-treated group in the PC1 direction (Figure 3D), suggesting that these compounds may counteract TGF- β 1 effects. Stained images showed that cells treated with CPT, DMC, ART, SNP and BER exhibited epithelial cell morphology, similar to that of the control group (Figure 3A). Representative staining images of the negative compounds are presented in Figure S1. The 5 compounds identified above thus altered the morphology of TGF- β 1-induced A549 cells and may have acted to inhibit or reverse the EMT.

3.4. Validation of anti-EMT activity of monomeric compounds

The TGF- β 1-induced EMT not only causes changes in morphology of lung epithelial cells but also in EMT-related markers and cell function. qRT-PCR and Western blotting analysis showed that the expression of E-cadherin was decreased whereas the expression of Vimentin and α -SMA was increased in the TGF- β 1-treated group compared with controls. Treatment with CPT, DMC, ART, SNP or BER decreased expression of Vimentin and α -SMA and increased that of E-cadherin relative to the TGF- β 1-treated group (Figure 4). Cell adhesion assays showed that the number of adherent cells was reduced by TGF- β 1-treatment compared with controls, a change that was partially reversed by treatment with CPT, DMC, ART, SNP or BER (Figure 5). Reduced scratch areas consistent

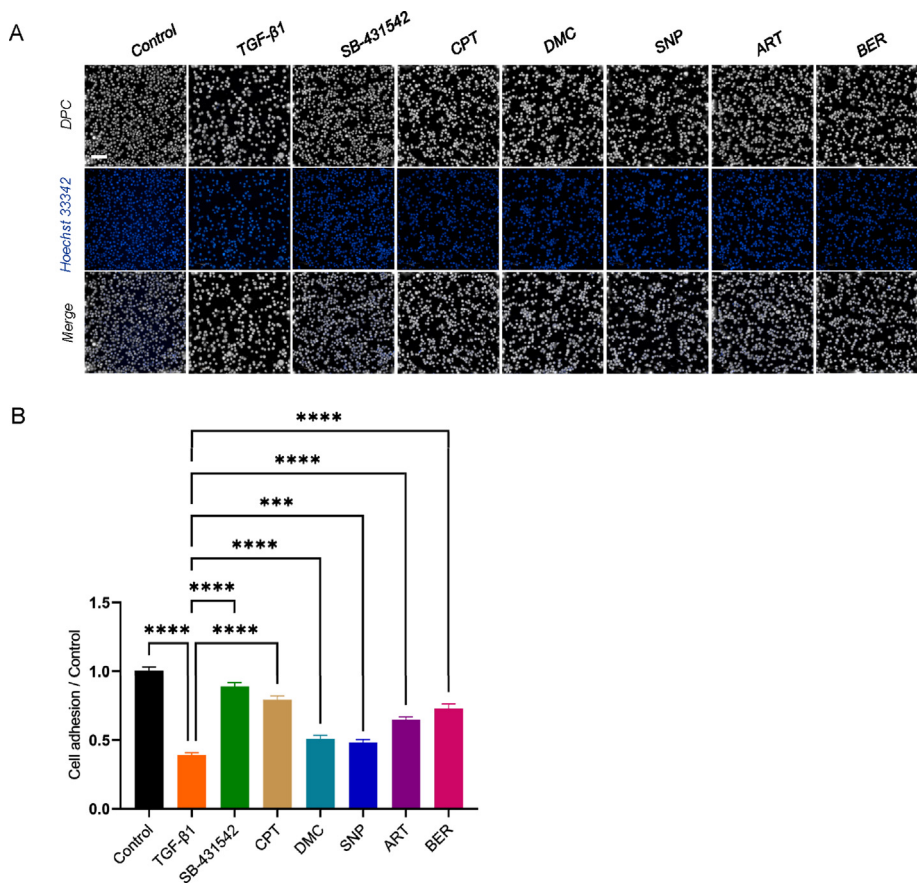


Figure 5. Adhesion of A549 cells following treatment with monomeric compounds. A549 cells were seeded into 6-well plates at a density of 3×10^5 cells/well. After 72 h, nuclei were stained with Hoechst 33342. Digital Phase Contrast (DPC) images were acquired using a $20 \times$ objective of the Opera Phoenix HCS system (Perkin Elmer). Images were identified and segmented using Harmony software to calculate numbers of adherent cells. (A) Representative stained cell adhesion images after incubation with different compounds. Scale bar = 100 μ m. (B) Adhesion of A549 cells after 72 h (means \pm SEM; n = 6; ***p < 0.001; ****p < 0.0001).

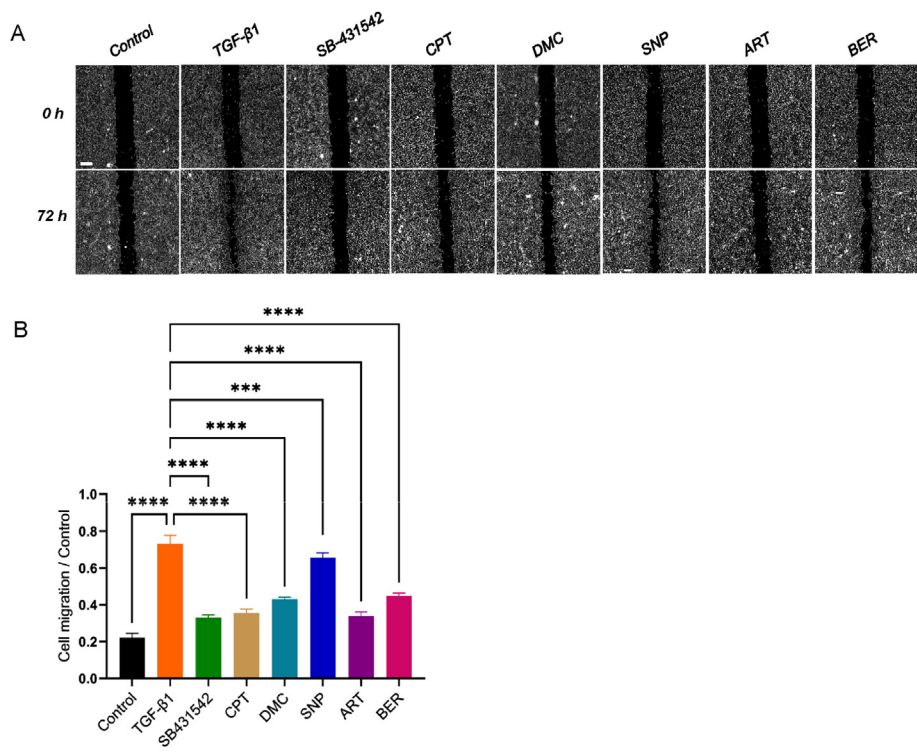


Figure 6. Migration of A549 cells following treatment with monomeric compounds. A549 cells were seeded into 6-well plates at a density of 5×10^5 cells/well. DPC images were acquired using a $10 \times$ objective of the Opera Phoenix HCS system (Perkin Elmer). Images were identified and segmented using Harmony software to calculate the area of cell migration. (A) Representative images of different experimental conditions at 0 h and 72 h. Scale bar = 1 mm (B) Changes in cell migration after 72 h (means \pm SEM; n = 6; ***p < 0.001; ****p < 0.0001).

with enhanced cell migration were seen for the TGF-β1-treated group compared with controls, a change that was also partially reversed by treatment with CPT, DMC, ART, SNP or BER (Figure 6). In summary,

these results indicate inhibition of the EMT, enhanced cell adhesion and reduced cell migration after treatment with CPT, DMC, ART, SNP or BER.

4. Discussion

TGF- β 1 induces epithelial cells to undergo morphological and functional alterations characteristic of the EMT. The cell cytoskeleton is reorganized and morphology changes from pebble-like to spindle-like [8, 9]. Subsequently, cells lose intercellular contacts and apical-basal polarity, gradually transforming into mesenchymal cells [5, 6, 7]. The loss of E-cadherin, accompanied by increased expression of Vimentin and α -SMA, makes the EMT a key driver of cancer cell spread and the invasive migration of fibrotic lesions [25, 26, 27]. Thus, the EMT is a key factor contributing to idiopathic pulmonary fibrosis (IPF) and to lung cancer (LC). The HCS system is a fast and highly selective tool capable of high throughput analysis. It allows comprehensive recording of phenotypic changes and quantifies different morphological parameters by segmenting cell images using intelligent algorithms. In recent years, HCS has been used for drug screening, virus infection, toxicology and tumor migration studies [28, 29, 30, 31, 32]. Therefore, HCS is an appropriate system for the quantification of cell morphological changes during the EMT allowing distinction of the inhibitory effects of different compounds on this process. TCM is ideal for targeting the EMT because of its low rates of adverse effects and low generation of drug dependence. However, TCM represents a complex mixture of components, making it difficult to identify active ingredients. Therefore, there has been a pressing need to screen TCM monomers and identify components with anti-EMT activities.

The current study applied the HCS system to quantify phenotypic changes in A549 cells using multiple parameters during the TGF- β 1-induced EMT. First, the optimal conditions for TGF- β 1-induced EMT in A549 cells were determined and the screening method validated using the TGF- β 1 receptor blocker, SB-431542. A total of 306 monomeric compounds from the MCE compound library were screened. Primary screening indicated 5 monomeric TCM compounds, CPT, DMC, ART, SNP and BER, which inhibited the TGF- β 1-induced EMT in A549 cells. Further experiments showed that CPT, DMC, ART, SNP and BER increased E-cadherin expression, decreased expression of Vimentin and α -SMA, enhanced cell adhesion and weakened cell migration. CPT, ART and BER have been previously reported to inhibit the EMT [33, 34, 35]. Identification of the inhibitory actions of DMC and SNP on the TGF- β 1-induced EMT in A549 cells is a novel finding. Looking for literature, we did not find the inhibitory effects of the other 301 monomers on EMT. Overall, the above compounds of TCM were screened by using the HCS system, which indicates that the screening method we established is reliable without false negative results.

In conclusion, we report the establishment of a rapid, reliable and high-throughput screening method based on the HCS system to assess cell morphology changes during the EMT. Five monomeric components of TCM were screened from 306 candidate compounds and shown to have anti-EMT activity. The application of these compounds to the treatment of EMT-related diseases should be evaluated in future studies.

Declarations

Author contribution statement

Mengzhen Xu: Performed the experiments; Contributed reagents, materials, analysis tools or data; Analyzed and interpreted the data; Wrote the paper.

Qinghua Cui: Contributed reagents, materials, analysis tools or data; Analyzed and interpreted the data; Wrote the paper.

Wen Su, Dan Zhang: Contributed reagents, materials, analysis tools or data; Analyzed and interpreted the data.

Jiaxu Pan, Xiangqi Liu: Analyzed and interpreted the data.

Zheng Pang, Qingjun Zhu: Conceived and designed the experiments; Contributed reagents, materials, analysis tools or data; Analyzed and interpreted the data; Wrote the paper.

Funding statement

Qingjun Zhu was supported by Natural Science Foundation of Shandong Province [No. ZR2020MH384], Shandong Province of Traditional Chinese Medicine Science and Technology Development Project [No. 2019-0040].

Zheng Pang was supported by the National Natural Science Foundation of China [No. 82002112].

This work was supported by Key Technology Research and Development Program of Shandong [No. 2020CXGC010505].

Data availability statement

Data included in article/supp. material/referenced in article.

Declaration of interests statement

The authors declare no conflict of interest.

Additional information

Supplementary content related to this article has been published online at <https://doi.org/10.1016/j.heliyon.2022.e10238>.

References

- [1] X. Dai, et al., Ascoclolin enhances the sensitivity of doxorubicin leading to the reversal of epithelial-to-mesenchymal transition in hepatocellular carcinoma, *Mol. Cancer Therapeut.* 15 (2016) 2966–2976.
- [2] S.Y. Loo, et al., Manganese superoxide dismutase expression regulates the switch between an epithelial and a mesenchymal-like phenotype in breast carcinoma, *Antioxidants Redox Signal.* 25 (2016) 283–299.
- [3] C.Y. Loh, et al., The E-cadherin and N-cadherin switch in epithelial-to-mesenchymal transition: signaling, therapeutic implications, and challenges, *Cells* 8 (2019).
- [4] D.P. Lavin, V.K. Tiwari, Unresolved complexity in the gene regulatory network underlying EMT, *Front. Oncol.* 10 (2020) 554.
- [5] R.Y. Huang, P. Guilford, J.P. Thiery, Early events in cell adhesion and polarity during epithelial-mesenchymal transition, *J. Cell Sci.* 125 (2012) 4417–4422.
- [6] S. Lamouille, J. Xu, R. Derynck, Molecular mechanisms of epithelial-mesenchymal transition, *Nat. Rev. Mol. Cell Biol.* 15 (2014) 178–196.
- [7] R. Chatterjee, J. Chatterjee, Ros and oncogenesis with special reference to EMT and stemness, *Eur. J. Cell Biol.* 99 (2020), 151073.
- [8] M. Yilmaz, G. Christofori, EMT, the cytoskeleton, and cancer cell invasion, *Cancer Metastasis Rev.* 28 (2009) 15–33.
- [9] R. Mayor, S. Etienne-Manneville, The front and rear of collective cell migration, *Nat. Rev. Mol. Cell Biol.* 17 (2016) 97–109.
- [10] H. Kasai, J.T. Allen, R.M. Mason, T. Kamimura, Z. Zhang, Tgf-Beta1 induces human alveolar epithelial to mesenchymal cell transition (EMT), *Respir. Res.* 6 (2005) 56.
- [11] J. Chen, C.B. Yuan, B. Yang, X. Zhou, Baicalin inhibits EMT through Pdk1/Akt signaling in human nonsmall cell lung cancer, *J. Oncol* 2021 (2021), 4391581.
- [12] L. Jin, et al., Gallic acid attenuates pulmonary fibrosis in a mouse model of transverse aortic contraction-induced heart failure, *Vasc. Pharmacol.* 99 (2017) 74–82.
- [13] J. Li, et al., Andrographolide attenuates epithelial-mesenchymal transition induced by tgf-beta1 in alveolar epithelial cells, *J. Cell. Mol. Med.* 24 (2020) 10501–10511.
- [14] S. Yang, et al., Astragalus polysaccharide inhibits breast cancer cell migration and invasion by regulating Epithelialmesenchymal transition via the Wnt/betacatenin signaling pathway, *Mol. Med. Rep.* 21 (2020) 1819–1832.
- [15] M. Boutros, F. Heigwer, C. Lauffer, Microscopy-based high-content screening, *Cell* 163 (2015) 1314–1325.
- [16] U.M. Mattiazzi, et al., High-content screening for quantitative cell biology, *Trends Cell Biol.* 26 (2016) 598–611.
- [17] K. Smith, et al., Phenotypic image analysis software tools for exploring and understanding big image data from cell-based assays, *Cell Syst* 6 (2018) 636–653.
- [18] I. Fraietta, F. Gasparri, The development of high-content screening (Hcs) Technology and its importance to drug discovery, *Expert Opin. Drug Discov.* 11 (2016) 501–514.
- [19] K.A. Foster, C.G. Oster, M.M. Mayer, M.L. Avery, K.L. Audus, Characterization of the a549 cell line as a type II pulmonary epithelial cell model for drug metabolism, *Exp. Cell Res.* 243 (1998) 359–366.
- [20] K. Hisatomi, et al., Pirfenidone inhibits Tgf-beta1-induced over-expression of collagen type I and heat shock protein 47 in a549 cells, *Bmc Pulm. Med.* 12 (2012) 24.
- [21] T. Yang, M. Chen, T. Sun, Simvastatin attenuates tgf-beta1-induced epithelial-mesenchymal transition in human alveolar epithelial cells, *Cell. Physiol. Biochem.* 31 (2013) 863–874.

- [22] J.H. Zhang, T.D. Chung, K.R. Oldenburg, A simple statistical parameter for use in evaluation and validation of high throughput screening assays, *J. Biomol. Screen* 4 (1999) 67–73.
- [23] B. Sangiorgi, et al., A high-content screening approach to identify micromas against head and neck cancer cell survival and EMT in an inflammatory microenvironment, *Front. Oncol.* 9 (2019) 1100.
- [24] S.K. Halder, R.D. Beauchamp, P.K. Datta, A specific inhibitor of Tgf-beta receptor kinase, Sb-431542, as a potent antitumor agent for human cancers, *Neoplasia* 7 (2005) 509–521.
- [25] R.K. Das, et al., Epithelio-mesenchymal transitional attributes in oral sub-mucous fibrosis, *Exp. Mol. Pathol.* 95 (2013) 259–269.
- [26] M. Ashrafzadeh, et al., Micromas and their influence on the Zeb family: mechanistic aspects and therapeutic applications in cancer therapy, *Biomolecules* 10 (2020).
- [27] Z. Wang, Y. Li, F.H. Sarkar, Signaling mechanism(S) of reactive oxygen species in epithelial-mesenchymal transition reminiscent of cancer stem cells in tumor Progression, *Curr. Stem Cell Res. Ther.* 5 (2010) 74–80.
- [28] G. Hilfenhaus, et al., A high-content screen identifies drugs that restrict tumor cell extravasation across the endothelial barrier, *Cancer Res.* 81 (2021) 619–633.
- [29] M.T. Donato, L. Tolosa, Application of high-content screening for the study of hepatotoxicity: focus on food toxicology, *Food Chem. Toxicol.* 147 (2021), 111872.
- [30] K. Rodriguez, et al., Evaluation of in vitro activity of copper gluconate against SARS-Cov-2 using confocal microscopy-based high content screening, *J. Trace Elem. Med. Biol.* 68 (2021), 126818.
- [31] D.A. Cardoso, N. Chau, P.J. Robinson, High-content drug discovery screening of endocytosis pathways, *Methods Mol. Biol.* 2233 (2021) 71–91.
- [32] M. Donato, L. Tolosa, High-content screening for the detection of drug-induced oxidative stress in liver cells, *Antioxidants (Basel)*. 10 (2021).
- [33] Z.Y. Wang, et al., Artesunate inhibits the development of Pvr by suppressing the Tgf-beta/smad signaling pathway, *Exp. Eye Res.* 213 (2021), 108859.
- [34] H. Du, et al., Berberine suppresses EMT in liver and gastric carcinoma cells through combination with Tgfbetar regulating Tgf-beta/smad pathway, *Oxid. Med. Cell. Longev.* 2021 (2021), 2337818.
- [35] Q. Liu, et al., Nrf2 down-regulation by camptothecin favors inhibiting invasion, metastasis and angiogenesis in hepatocellular carcinoma, *Front. Oncol.* 11 (2021), 661157.